Journal of Biomedical Optics

BiomedicalOptics.SPIEDigitalLibrary.org

# Diffusion characteristics of ethylene glycol in skeletal muscle

Luís M. Oliveira
Maria Inês Carvalho
Elisabete M. Nogueira
Valery V. Tuchin

SPIE.

Journal of Biomedical Optics 20(5), 051019 (May 2015)

# Diffusion characteristics of ethylene glycol in skeletal muscle

**Luís M. Oliveira,[a,b,c,*] Maria Inês Carvalho,[d,e] Elisabete M. Nogueira,[a,c] and Valery V. Tuchin[f,g,h]**
[a]Polytechnic of Porto, School of Engineering, Physics Department, Rua Dr. António Bernardino de Almeida, 431, 4200-072 Porto, Portugal
[b]Porto University, School of Engineering, Rua Dr. Roberto Frias, 4200-465 Porto, Portugal
[c]Centre of Innovation in Engineering and Industrial Technology, ISEP, Rua Dr. António Bernardino de Almeida, 431, 4200-072 Porto, Portugal
[d]Porto University, School of Engineering, DEEC, Rua Dr. Roberto Frias, 4200-465 Porto, Portugal
[e]INESC TEC, FEUP, Rua Dr. Roberto Frias, 4200-465 Porto, Portugal
[f]Saratov State University, Research-Educational Institute of Optics and Biophotonics, 83, Astrakhanskaya Street, Saratov 410012, Russia
[g]Institute of Precise Mechanics and Control RAS, Laboratory of Laser Diagnostics of Technical and Living Systems, 24 Rabochaya Street, Saratov 410028, Russia
[h]University of Oulu, Optoelectronics and Measurement Techniques Laboratory, PO Box 4500, 90014 Oulu, Finland

**Abstract.** Part of the optical clearing study in biological tissues concerns the determination of the diffusion characteristics of water and optical clearing agents in the subject tissue. Such information is sufficient to characterize the time dependence of the optical clearing mechanisms—tissue dehydration and refractive index (RI) matching. We have used a simple method based on collimated optical transmittance measurements made from muscle samples under treatment with aqueous solutions containing different concentrations of ethylene glycol (EG), to determine the diffusion time values of water and EG in skeletal muscle. By representing the estimated mean diffusion time values from each treatment as a function of agent concentration in solution, we could identify the real diffusion times for water and agent. These values allowed for the calculation of the correspondent diffusion coefficients for those fluids. With these results, we have demonstrated that the dehydration mechanism is the one that dominates optical clearing in the first minute of treatment, while the RI matching takes over the optical clearing operations after that and remains for a longer time of treatment up to about 10 min, as we could see for EG and thin tissue samples of 0.5 mm.  [DOI: 10.1117/1.JBO.20.5.051019]

Keywords: optical clearing; agent diffusion; diffusion coefficient; collimated transmittance; tissue dehydration; refractive index matching.

Paper 140473SSR received Jul. 24, 2014; accepted for publication Nov. 21, 2014; published online Dec. 19, 2014; corrected Feb. 18, 2015.

## 1 Introduction and Motivation

The study of drug and fluid diffusions and delivery into biological tissues represents an important research field with applications in different areas like clinical practice, pharmacology, and cosmetics. Moreover, the study of fluid diffusion is also of the greatest importance in biophotonics research,[1] since the diffusion of fluids is at the basis of the mechanisms that compose the optical immersion clearing method. In effect, most biological tissues present a characteristic high-scattering coefficient and consequently are considered turbid to the passage of light. Such high-scattering coefficients are observed not only by the existence of discrete scatterer elements inside the tissues, but also due to the significant difference between the refractive index (RI) values of these scatterers and of the surrounding media—the interstitial fluid.[2] Such significant light scattering in biological tissues is a major inconvenience when optical technologies are applied to perform diagnosis or treatment procedures, since light scattering limits tissue depth and beam collimation.[2–6] A potential method to reduce light scattering in biological tissues is the optical immersion clearing method, which allows reaching higher tissue depths with higher beam collimation through the creation of a temporary transparency effect in the tissue. Such improvement in the optical beam inside the tissue will make possible deeper laser surgery and deeper optical image acquisition for a diagnosis.[7] The various research studies done so far with this method have used different types of biological tissues and optical clearing agents (OCAs) to obtain the decreased light scattering during the applied treatments.[7–18] The transparency effect initiates with the administration of an OCA to the tissue, which can be made topically or by tissue immersion in the agent. Once the OCA enters in contact with the tissue, the optical transparency effect is created through the cooperation of two mechanisms: tissue dehydration and RI matching.[18] As an example, when an *ex vivo* tissue sample is immersed in a solution that contains an active OCA, an osmotic pressure will be created over the sample, forcing it to lose water from the interstitial space, and consequently originating a lesser sample thickness and better ordering of tissue scatterers. On the other hand, the OCA in the immersing solution will diffuse into the sample and place itself in the interstitial locations, close to the scatterers. Since OCAs present a higher RI than water and are closer to the RI of the tissue scatterers like mitochondria, tissue cells, organelles, or muscle fibers, the partial replacement of the interstitial water by the OCA provides the RI matching mechanism and consequently decreases light scattering inside the tissue.[18] The dehydration mechanism described above considers that the water flows from the *ex vivo* tissue sample to the environment permanently. In the case of *in vivo* study, the dehydration mechanism is not so simple, since the tissue under study is

*Address all correspondence to: Luís M. Oliveira, E-mail: lmo@isep.ipp.pt

1083-3668/2015/$25.00 © 2015 SPIE

in biological contact with adjacent tissues and the water content in the surrounding tissues might limit the loss of water in the tissue under study. From the previous description and considering the *ex vivo* study, we see that during optical clearing there will be a flux of water out of the tissue sample and a flux of OCA into the tissue. These two fluxes are associated with the two mechanisms of optical clearing, but they do not occur independently. For this reason, it is important to find a way to characterize both of these fluxes and discriminate one from the other.

Here, as part of our research regarding the optical clearing of *ex vivo* skeletal muscle samples with different OCAs, we have used a simple method to estimate the diffusion properties of OCAs and water to discriminate between the two fluxes. By obtaining such data, we could present a more detailed characterization of the optical clearing effects created. Our objective in the present study was to validate the simple and innovative method to determine the diffusion properties of OCAs in biological tissues. In this study, we have used ethylene glycol (EG) to perform the optical clearing treatments of the muscle samples.

This paper is organized as follows. Section 2 presents the theoretical fundamentals of the method used in our research, the preparation of the muscle samples, and OCA solutions to be used in the experiments. Section 3 presents the results obtained and the discussion of those results. Section 4 presents the final conclusions of our research.

## 2 Materials and Methods

### 2.1 *Methods*

The diffusion of OCAs in biological tissues and blood *in vitro* and *in vivo* has been studied by several researchers using different methods.[19–23] There are two parameters that characterize the diffusion of an OCA in a biological tissue—the diffusion time and the diffusion coefficient. These parameters are different for each combination tissue/OCA and their determination is most significant to help in characterizing the optical clearing effect created. Some publications have reported the diffusion time for some OCAs such as dimethyl sulfoxide,[24] glucose,[19,21,25] manitol,[21] sucrose,[26] glycerol,[4] lactose, and fructose[26] in different biological tissues and phantoms. On the other hand, a recent publication shows the results from a study of glucose diffusion permeability in normal and cancerous esophageal tissues.[20] Different studies to evaluate OCA concentration efficiency with tissue depth and improved contrast of optical coherence tomography or second-harmonic generation images at deeper tissue layers have also been reported.[3,5,27,28] Mathematical models have also been developed to describe OCA diffusion in biological tissues.[1,18,25,29]

The method that we have selected to study and discriminate between the two diffusion fluxes of OCA and water during optical clearing is based on collimated transmittance measurements. Due to the nature of these measurements, our study is reported for *in vitro* samples. Such a method allows the estimation of the characteristic diffusion time and diffusion coefficient both for OCA and water and is well described in literature.[1,6,18]

To characterize the water and OCA fluxes created by an optical immersion treatment of the skeletal muscle, we consider the muscle sample to have a slab form with thickness $d$. When this *ex vivo* sample is immersed in an aqueous solution containing an OCA, the agent diffuses from the environment into the sample through both surfaces of the slab at the same time. Such a type of diffusion is described by Fick's law of diffusion:[1,18,30–32]

$$\frac{\partial C_a(x,t)}{\partial t} = D_a \frac{\partial^2 C_a(x,t)}{\partial t^2}. \tag{1}$$

Equation (1) characterizes the time dependence of the agent concentration $C_a$ at any unidirectional position $x$ between the two surfaces of the tissue slab. The diffusion coefficient of the agent inside the tissue is represented in Eq. (1) as $D_a$.[18] Such a coefficient is related to the diffusion time of the agent in the tissue by Eq. (2) for a diffusion occurring through both slab surfaces:[1,18,30,31]

$$\tau = \frac{d^2}{\pi^2 D_a}. \tag{2}$$

Assuming that the volume of the solution used is significantly higher than the volume of the slab sample (e.g., 10×), the amount of the dissolved matter $m_t$ in the tissue at an instant $t$ relative to its equilibrium value $m_\infty$ can be determined by Eq. (3):[18,31]

$$\frac{m_t}{m_\infty} = \frac{\int_0^d C_a(x,t)\mathrm{d}x}{C_{a0}d} = 1 - \frac{8}{\pi^2}\left[\exp\left(-\frac{t}{\tau}\right) + \frac{1}{9}\exp\left(-\frac{9t}{\tau}\right) + \frac{1}{25}\exp\left(-\frac{25t}{\tau}\right) + \ldots\right]. \tag{3}$$

The ratio presented in Eq. (3) represents the volume averaged concentration of an agent $C_a(t)$ that is located inside the slab sample at a particular time $t$. The solution of Eq. (3) using a first-order approximation is given by[1,18,32]

$$C_a(t) = \frac{1}{d}\int_0^d C_a(x,t)\mathrm{d}x \cong C_{a0}\left[1 - \exp\left(-\frac{t}{\tau}\right)\right]. \tag{4}$$

Equation (4) provides a relation between the time dependence of the agent's concentration within the sample and the characteristic diffusion time of the agent inside the sample.[33] If we use this characteristic diffusion time $\tau$ in Eq. (2), we can calculate the corresponding diffusion coefficient. These are the two parameters that we want to estimate for the optical clearing of biological samples. We have to note that Eqs. (1)–(4) are valid for the description of free diffusion of one type of molecules in a medium. When two fluxes are induced in the system, such as OCA flux directed into the tissue and water flux out, these equations can also be applicable, but the diffusion coefficient $D_a$ or the diffusion time $\tau$ in that case will characterize diffusivity of both fluxes in accordance with strengths of each of these fluxes.

If we use a spectrometer and a broadband light source to perform collimated transmittance ($T_c$) measurements from a slab muscle sample during optical clearing immersion treatment with an aqueous solution that contains an active OCA in a particular concentration, then it is possible to create a time dependence for $T_c$ for various wavelengths. Each of the individual time dependencies can be fitted with lines that are described mathematically in accordance with Eq. (4), since the $T_c$ time dependence translates the two fluxes. When the fittings are made for each of the wavelengths, we obtain the characteristic diffusion

time of the mixed agent/tissue water fluxes within the tissue. The mean diffusion time obtained from each of the fittings can be calculated for that particular treatment. By repeating this procedure for other treatments with different concentrations of agent in the immersing solution, we will obtain a collection of diffusion times that can be represented as a function of OCA concentration in solution. Such data can be fitted with a smooth line to estimate the dependence between the diffusion time and agent concentration in solution. If the agent's concentrations in solution are well chosen, then we will be able to retrieve valuable information from the fitting line as we have already observed in our previous study with glucose solutions.[33] In that study, we have observed that the fitting line presents a peak for a concentration of 40.5% of glucose in the immersing solution. Such a peak indicates optimal diffusion of glucose into the muscle for this concentration due to the equilibrium verified for this agent concentration between tissue-free water and the immersing solution water. This means that we were also able to identify the amount of free water in the skeletal muscle as 59.5% of the sample volume. On the other hand, the magnitude of the peak indicates the true diffusion time value of the OCA in the muscle. Such value can then be used in Eq. (2) to calculate the diffusion coefficient of the agent in the tissue. In opposition to this particular treatment that verifies the water equilibrium between tissue and immersing solution, highly concentrated solutions have low water content. For those nearly saturated solutions, the water content is practically null and the effect seen in the $T_c$ time dependence corresponds only to water diffusion related to the dehydration mechanism of optical clearing. Such a fact is created by the large OCA content in the immersing solution, which provides a strong osmotic pressure over the tissue sample, forcing water to flow out without the occurrence of agent flux into the tissue. Using the same methodology as in the study with glucose solutions,[33] we now present here a similar study performed with solutions of EG that were used to treat skeletal muscle samples. Our purpose is to compare results obtained from the studies performed with both agents for validation. EG cannot be considered as an OCA to be used for clinical procedures, since it is a toxic alcohol that originates several pathological changes if in contact with different biological tissues.[34] On the other hand, if we are interested in acquiring information to be used in treatment procedures related to accidental exposure, then the diffusion study of EG in the muscle can prove itself valuable.

Considering the data already collected from the study with glucose solutions, we have elected to perform a similar study with EG solutions to characterize its diffusion in the skeletal muscle and to compare results with the study with glucose. The following subsections contain information about the EG solutions, the muscle samples, and the methodology used in our experiments.

### 2.2 *Muscle Samples*

We have selected the abdominal wall muscle from the Wistar Han rat to use in our studies. A single animal was sacrificed and the entire abdominal wall muscle was dissected from the animal. By slicing all the samples from this unique muscle block, we have guaranteed a maximum physiological similarity between samples used in all studies. We have prepared smaller samples from the muscle block with a circular-slab form and a diameter of approximately 10 mm. These samples were sliced at a cryostat with a thickness of 0.5 mm. The volume of the samples was 39.27 $mm^3$. We have prepared nine samples with this thickness to be used in the experimental studies.

### 2.3 *Ethylene Glycol Solutions*

To perform the optical clearing treatments, we have prepared several aqueous solutions with different concentrations of EG. We have diluted commercial EG with 99% purity in distilled water to prepare the various solutions to be used in the various treatments. Similarly to our previous study with glucose solutions,[33] we have prepared the EG solutions in the following concentrations: 20%, 25%, 30%, 35%, 40%, 45%, 50%, 55%, and 60%. An independent study was performed for muscle samples under treatment with each of these solutions. The preparation of these solutions was controlled by the measurement of the RI of the solution with an Abbe refractometer. According to available experimental data,[35] aqueous solutions of EG have an RI of 589.6 nm at 20°C, that is described by

$$n_{\mathrm{EGw}} = 0.001 \times C_{\mathrm{EG}} + 1.3326. \tag{5}$$

The RI values measured by the Abbe refractometer also refer to 589.6 nm. We have used Eq. (5) to calculate the RI values for the desired solutions. These calculated RI values are presented in Table 1. Using these calculated values as reference, we have mixed EG and water until the RI value measured on the Abbe refractometer was the same as the one calculated for each solution.

### 2.4 *Experimental Methodology*

In each of the treatments that we have performed, the collimated transmittance spectra were measured from the samples with the experimental assembly represented in Fig. 1.

The setup presented in Fig. 1 is in cross section. The glass that is placed below the sample has a 1-mm thickness and it is used to create a cuvette to sustain the optical clearing solutions during the treatments. The illumination beam presented at the bottom in Fig. 1 is delivered by an optical fiber cable and collimating lens, and it presents a diameter of 6 mm below the glass. Such a beam comes from a tungsten-halogen lamp (model HL-2000 from Avantes Corporation™—wavelength range from

**Table 1** Optical clearing solutions.

| Concentration of ethylene glycol (EG) (%) | Refractive index (RI) |
|---|---|
| 20 | 1.3525 |
| 25 | 1.3576 |
| 30 | 1.3626 |
| 35 | 1.3676 |
| 40 | 1.3725 |
| 45 | 1.3776 |
| 50 | 1.3825 |
| 55 | 1.3876 |
| 60 | 1.3925 |

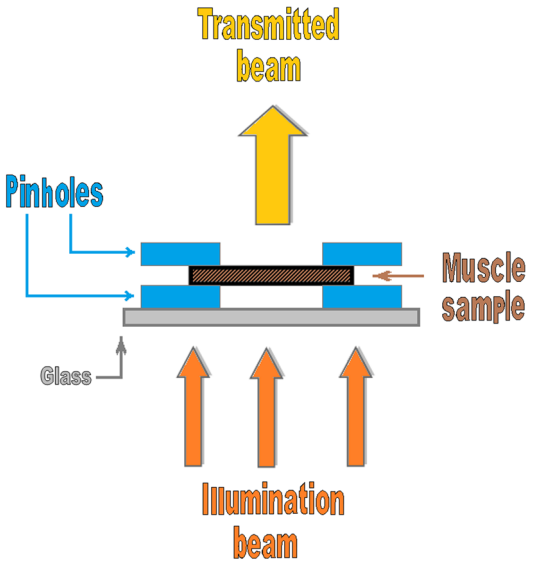


**Fig. 1** Experimental setup to measure the collimated transmittance.

360 to 2000 nm) and the spectra measured from this setup are acquired with an AvaSpec-2048-USB2 spectrometer, also from Avantes. This spectrometer has a grating set for 200 to 1100 nm and a 50-$\mu$m slit.

We have initiated the measurements for each treatment by measuring the reference spectrum from the light source. Such a reference spectrum was acquired with the same setup as represented in Fig. 1, but without the sample placed at the center.

After acquiring the reference spectrum from the light source, we have placed the muscle sample at the center of the setup presented in Fig. 1 and have acquired the natural collimated transmitted spectrum. The measurements of collimated transmitted spectra of the muscle sample under treatment were performed after the solution was applied around the sample. The delivery of the immersing solution is made with a syringe through a lateral hole of the sample chamber (not seen on Fig. 1). Using this method and injecting the solution smoothly, it spreads immediately inside the chamber, below and above the muscle sample. The volume of the solution used was 10× the volume of the sample. The solution is sustained around the sample by the cuvette created by the glass and lateral walls presented in Fig. 1.

Since we have measured both the reference and collimated transmitted spectra from the sample, we had to calculate the collimated transmittance spectra for the natural sample and for different times of treatment. To perform such calculations, we have used Eq. (6):

$$T_c(\lambda, t) = \frac{T_{tc}(\lambda, t)}{S_{tc}(\lambda)}. \tag{6}$$

In Eq. (6), $T_{tc}(\lambda, t)$ represents the collimated transmitted spectrum measured from the sample at a particular time of treatment, $t$. The correspondent spectrum for the natural sample is represented as $T_{tc}(\lambda, t = 0)$. The reference spectrum, measured from the illumination beam and without the sample, is represented in Eq. (6) as $S_{tc}(\lambda)$.[33]

After obtaining all the spectra for a particular treatment, we have calculated the time dependencies of $T_c$ for a collection of wavelengths between 600 and 800 nm, the band where the skeletal muscle presents significant scattering.[33] Those time dependencies were first displaced vertically to have $T_c = 0$ at $t = 0$ s, and then they were normalized entirely to the highest value observed in the time dependence. After performing these adjustments, we have fitted these time dependencies with curves that have equations like Eq. (4), but with a small correction—we have normalized the concentration of agent in the tissue to the concentration of agent in the immersing solution so it can mimic the displaced and normalized $T_c$ time dependence data:

$$T_c(\lambda, t) = \frac{C_a(t)}{C_{a0}} \cong \left[1 - \exp\left(-\frac{t}{\tau}\right)\right]. \tag{7}$$

When performing these fittings, we have obtained the diffusion time value for each wavelength, $\tau(\lambda)$. We calculated the mean of the diffusion time for each treatment from the various diffusion time values obtained from the individual time dependencies of each wavelength.

Such methodology was repeated for the treatments with each optical clearing solution. After calculating all the mean diffusion time values for each treatment, we have represented the mean diffusion time as a function of the concentration of EG in the immersion solution. Such a representation was then fitted with a natural spline with the objective of characterizing the diffusion process. The results obtained using these methodologies are presented in the next section.

## 3 Results and Discussions

As we have indicated in Sec. 2, we have prepared the muscle samples with slab geometry with a thickness of 0.5 mm and the optical clearing solutions with the desired concentrations of EG. Using Eq. (5), we have calculated the RI values for the EG solutions, which were used as a reference in the preparation of these solutions through the control measurement with the Abbe refractometer (Table 1).

The RI values presented in Table 1 have a precision of four digits, but our Abbe refractometer only gives a precision of three digits. This means that we have optimized the immersion solutions by measuring the RI in the refractometer as close as possible to the values presented in Table 1. With this method of visually measuring the RI of the solution in the Abbe refractometer, our final solutions have the same RI as presented in Table 1, but with an uncertainty of $\pm 0.0005$.

Using these solutions and the experimental assembly represented in Fig. 1, we have measured the spectra from the reference beam and from the sample and calculated the collimated transmittance spectra for the natural muscle and for the sample under treatment with each solution according to Eq. (6). Figure 2 presents the $T_c$ spectrum of the natural skeletal muscle and Fig. 3 presents the time dependence of $T_c$ for wavelengths between 400 and 1000 nm for all treatments studied.

As we can see from the graphs in Fig. 3, the time dependence of $T_c$ does not show a smooth behavior for all treatments. For the treatment with a concentration of 40% of EG, we see that smooth behavior. This fact indicates that for this concentration, or for a concentration near 40%, EG has an optimized diffusion into the muscle.

For the treatments with EG in concentrations lower than 40%, we see a very fast increase within the first 2 min of the treatment followed by a saturation regime that is maintained for a few minutes, before presenting a decreasing behavior at the end of the treatment. The time period for the saturation

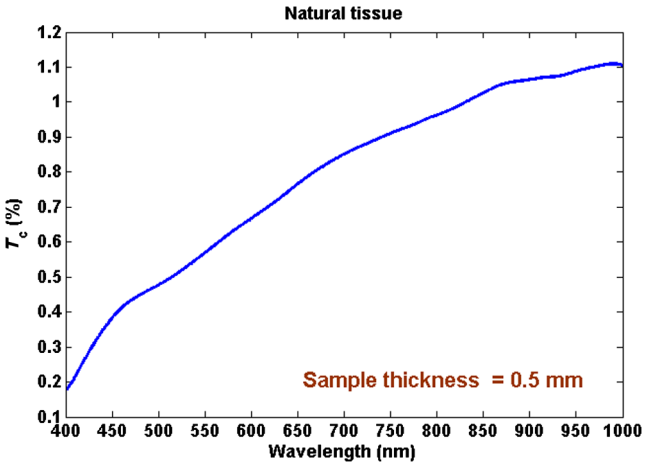


**Fig. 2** Collimated transmittance of the natural skeletal muscle from the Wistar Han rat.

regime increases with increasing concentration of EG in solution, as we can see from graphs in Figs. 3(a) through 3(e). After the saturation regime, $T_c$ shows a decreasing behavior, indicating that the sample has increased its thickness or has lost some EG to the outside. The magnitude of such a final decrease is higher for lower concentrated solutions.

For the treatments with solutions containing concentrations of EG higher than 40%, we see that, as the concentration of EG increases, the initial rise in $T_c$ tends to become contained in the first 2 min of treatment once more. This fact indicates that as the concentration of EG increases in the immersion solution, the dehydration mechanism tends to dominate the optical clearing operations due to a higher osmotic pressure created over the tissue by the agent. After this initial increase, we again see the saturation regime, which tends to take less time as the concentration of agent increases to give place to a second-step diffusion of EG into the tissue. This second-step diffusion of the agent into the muscle shows a higher increasing behavior for the higher concentrated solutions.

According to the methodology that we have described in Sec. 2, to estimate the mean diffusion time for each treatment, we have considered time dependence curves like the ones presented in Fig. 3, but only for wavelengths between 600 and 800 nm, the band where the muscle presents more scattering. We have displaced each of those curves to have $T_c = 0$ at $t = 0$ (natural tissue). After that we have normalized each curve to its highest value, which corresponds to the beginning of the saturation regime. Figure 4 shows the displaced curves for the various treatments and wavelengths, but without considering the normalization procedure for better visual perception.

Although the graphs presented in Fig. 4 are not normalized, they provide some important information. The first piece of information retrieved from these graphs regards the treatment duration until the first stage of saturation begins. This time period varies from case to case as we can see by the upper time limit in each graph of Fig. 4. By analyzing each graph of Fig. 4, we see that as the concentration of EG rises, the time limit of the graph increases until a concentration of 40% of EG is used. For concentrations higher than 40%, the inverse behavior is seen—the upper time limit of the graph lowers with the rising concentration of EG in solution. This information is very important, since it indicates which mechanism dominates the optical clearing treatment for each concentration of EG in solution. For concentrations of EG lower and higher than 40%, the dehydration mechanism dominates the optical clearing operations and for concentrations near 40%, the RI matching mechanism dominates. The optimal concentration of EG in solution is very close to 40%, as we have already observed in our previous study with glucose solutions.[33]

After performing normalization to the highest value in each case, each dataset from graphs in Fig. 4 was adjusted with an equation in the form of Eq. (7) to determine the diffusion time for each wavelength within the same treatment. Considering all the treatments studied, we presented in Table 2 the diffusion time values obtained for each curve for a particular treatment and the corresponding mean diffusion time for that treatment.

After calculating the mean diffusion time values for each treatment, we have represented these values as a function of EG concentration in solution. Such a representation is shown in Fig. 5 along with the natural spline that was calculated to fit the data points. Figure 5 also contains the results from the study with glucose solutions for comparison.[33]

The dashed curve in Fig. 5 shows that the diffusion of EG inside the skeletal muscle is maximal for a concentration of 40.5% of EG in the immersion solution. The same concentration was observed from the data obtained in the glucose study (solid line in Fig. 5). This means that for a solution containing that particular concentration of agent, no effective net water flux between the tissue and surrounding solution is observed and the only effective flux is one of the agents from the solution into the muscle. In that case, the agent flux is maximized. This result is observed in both datasets of Fig. 5. This result means that the free water content in the muscle tissue is the same water content in the solutions that present 40.5% concentration of agent: EG or glucose and possibly for others. That water content is 59.5%. Such a value of the free water content for the rat skeletal muscle is the same as the mean data indicated in literature for human, rabbit, and rat muscle samples.[36] This value is very important in the field of optical clearing, since it is the water portion that is free to move during the dehydration mechanism. Considering this data, we can calculate the bound water content in the muscle as 16.1%, which is the difference between total water (75.6%)[37,38] and free water (59.5%). The bound water portion is tightly connected to the other tissue components and does not participate in the optical clearing procedure, at least for a 30-min treatment.

The diffusion time of EG inside the muscle is also determined from the graph in Fig. 5. It corresponds to the value observed at the peak of the spline curve. This way, from the graph presented in Fig. 5, we obtain a diffusion time of 446.0 s for EG in the muscle, while for glucose we have only 302.9 s. For a particular treatment of muscle with solutions of EG or glucose in any concentration, we can calculate the concentration of the OCA inside the tissue as time dependent by using these diffusion time values in Eq. (4).

Considering that the diffusion of EG into the muscle was made through both surfaces of the tissue slab, we can apply Eq. (2) to calculate the diffusion coefficient of EG in the muscle:

$$D_{\mathrm{EG}} = \frac{d^2}{\pi^2 \tau_{\mathrm{EG}}} = \frac{0.045^2}{\pi^2 \times 446.0} = 4.60 \times 10^{-7}\ \mathrm{cm}^2/\mathrm{s}. \qquad (8)$$

In Eq. (8), $d$ represents the sample thickness at the time of treatment that corresponds to the maximum diffusion seen in

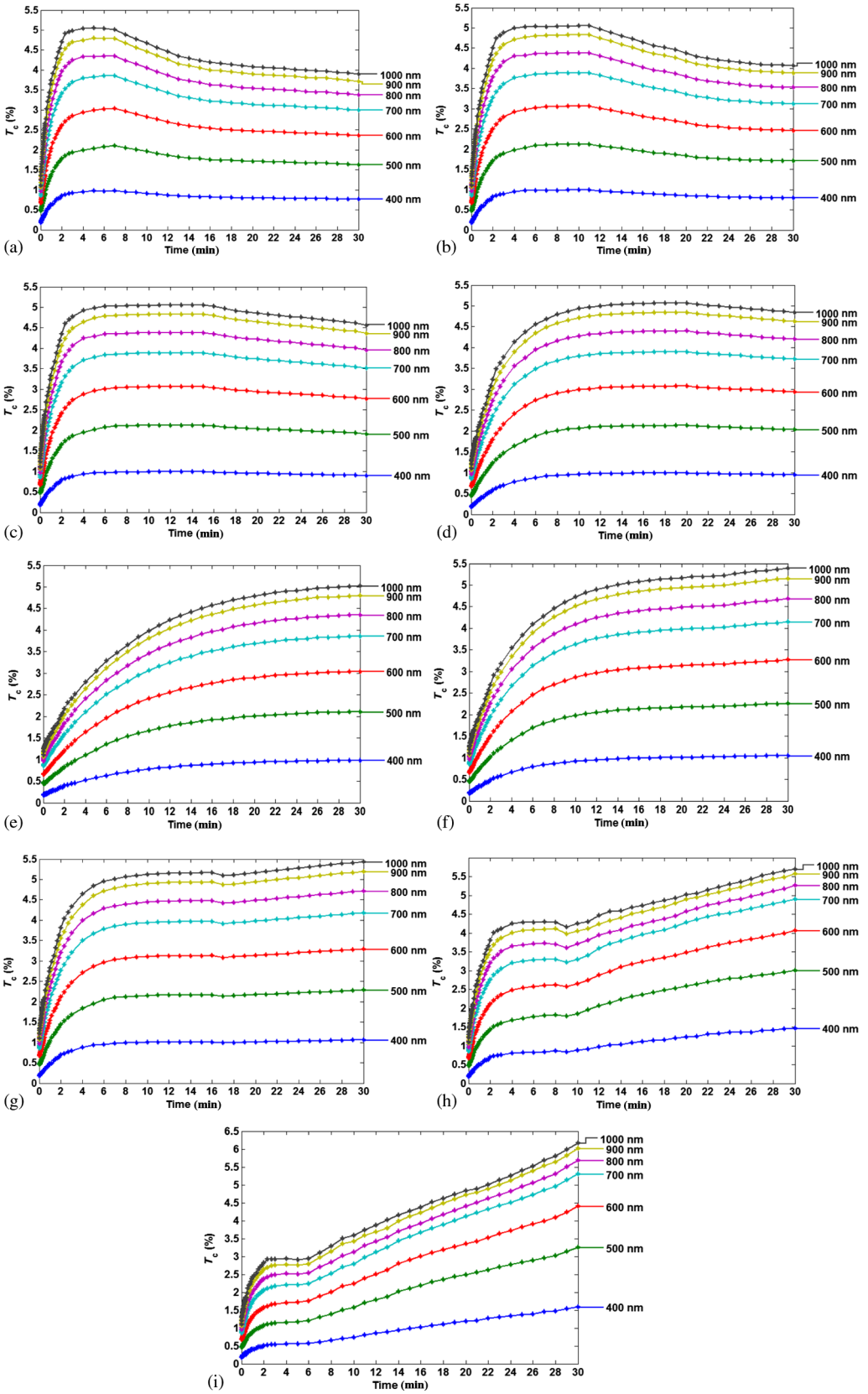


**Fig. 3** Time dependence of $T_c$ for several wavelengths from treatments of skeletal muscle samples from the Wistar Han rat with ethylene glycol (EG) of different concentrations: (a) 20%, (b) 25%, (c) 30%, (d) 35%, (e) 40%, (f) 45%, (g) 50%, (h) 55%, and (i) 60%.

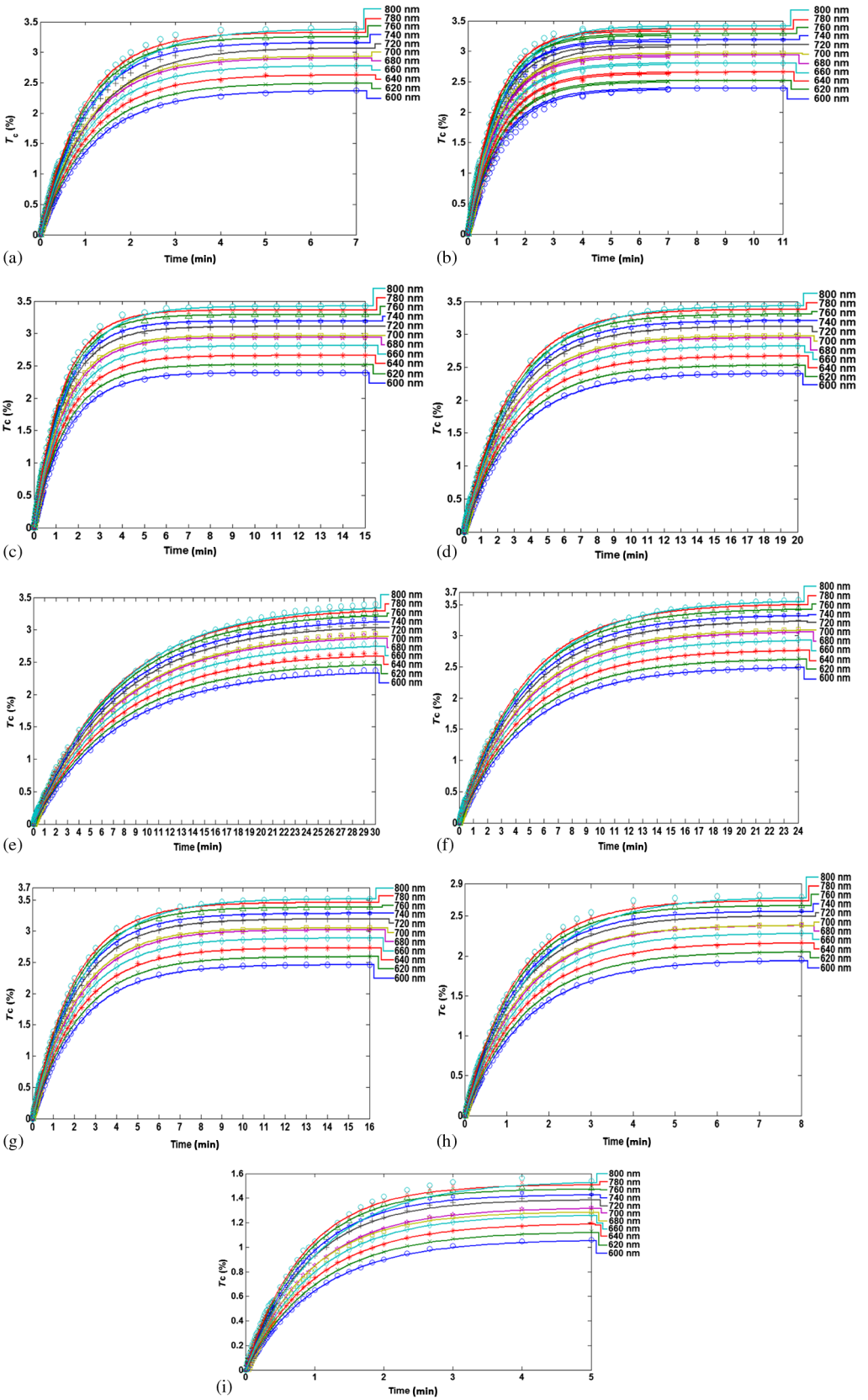


**Fig. 4** Time dependence $T_c$ data for wavelengths between 600 and 800 nm displaced to zero at $t = 0$ from treatments of skeletal muscle samples from the Wistar Han rat with EG of different concentrations: (a) 20%, (b) 25%, (c) 30%, (d) 35%, (e) 40%, (f) 45%, (g) 50%, (h) 55%, and (i) 60%.

**Table 2** The diffusion time experimental values.

| EG solution (%) | Wavelength (nm) | 600 | 620 | 640 | 660 | 680 | 700 | 720 | 740 | 760 | 780 | 800 |
|---|---|---|---|---|---|---|---|---|---|---|---|---|
| 20 | $\tau$ (s) | 70.1 | 68.2 | 66.6 | 65.6 | 64.3 | 62.6 | 69.9 | 59.6 | 58.7 | 57.9 | 70.1 |
| | Mean $\pm$ sd (s) | | | | | | $64.9 \pm 4.6$ | | | | | |
| 25 | $\tau$ (s) | 83.3 | 81.2 | 79.4 | 78.2 | 76.7 | 74.8 | 73.0 | 71.5 | 70.4 | 69.5 | 83.3 |
| | Mean $\pm$ sd (s) | | | | | | $76.5 \pm 5.0$ | | | | | |
| 30 | $\tau$ (s) | 92.6 | 90.3 | 88.4 | 87.1 | 85.6 | 83.6 | 81.5 | 79.9 | 78.7 | 77.8 | 92.6 |
| | Mean $\pm$ sd (s) | | | | | | $85.3 \pm 5.5$ | | | | | |
| 35 | $\tau$ (s) | 189.9 | 186.6 | 183.9 | 182.0 | 179.8 | 177.0 | 174.0 | 171.4 | 169.4 | 168.0 | 189.9 |
| | Mean $\pm$ sd (s) | | | | | | $179.3 \pm 7.9$ | | | | | |
| 40 | $\tau$ (s) | 450.9 | 448.3 | 446.2 | 444.5 | 442.6 | 440.7 | 438.8 | 436.4 | 433.9 | 432.7 | 450.9 |
| | Mean $\pm$ sd (s) | | | | | | $442.4 \pm 6.4$ | | | | | |
| 45 | $\tau$ (s) | 293.7 | 290.4 | 287.7 | 285.8 | 283.6 | 280.9 | 278.1 | 275.3 | 272.9 | 271.5 | 293.6 |
| | Mean $\pm$ sd (s) | | | | | | $283.0 \pm 8.0$ | | | | | |
| 50 | $\tau$ (s) | 137.9 | 135.0 | 132.6 | 131.1 | 129.1 | 126.6 | 124.1 | 121.9 | 120.3 | 119.1 | 137.9 |
| | Mean $\pm$ sd (s) | | | | | | $128.7 \pm 6.8$ | | | | | |
| 55 | $\tau$ (s) | 89.9 | 88.0 | 86.0 | 84.3 | 82.3 | 79.9 | 77.4 | 75.2 | 73.7 | 73.1 | 89.9 |
| | Mean $\pm$ sd (s) | | | | | | $81.8 \pm 6.3$ | | | | | |
| 60 | $\tau$ (s) | 64.4 | 63.0 | 61.6 | 60.2 | 58.2 | 56.0 | 54.0 | 52.6 | 51.5 | 50.7 | 64.4 |
| | Mean $\pm$ sd (s) | | | | | | $57.9 \pm 5.2$ | | | | | |

Fig. 5. For the case of EG, this time is 446 s and a thickness of 0.045 cm was obtained from a sample under treatment with EG 40% at the time of treatment of 446 s. For the study with glucose, we have done a similar calculation using the diffusion time of 303 s and the sample thickness measured at that particular time (0.042 cm) under treatment with glucose 40%. The calculated diffusion coefficient for glucose in the skeletal muscle is $5.90 \times 10^{-7}$ cm$^2$/s.

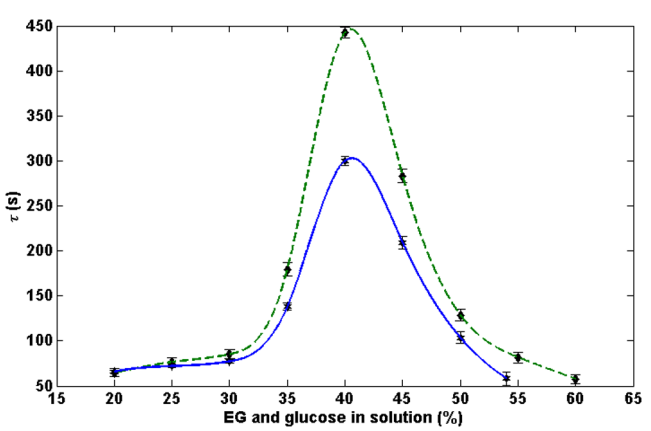


**Fig. 5** Mean diffusion time of EG versus EG concentration in solution: EG study—dashed line; glucose study—solid line (data taken from Ref. 33).

In addition to this information, we can also determine the diffusion time and the diffusion coefficient of water in the muscle from the graph of Fig. 5. To do that we will consider the diffusion time value observed for the highest concentrated solution of EG—EG 60%. For the treatment with this highly concentrated solution, we have an initial fast rise in the $T_c$ time dependence in Fig. 3(i), which occurs before the first saturation regime. In this treatment and since the immersion solution is highly saturated with EG, the agent in the solution creates an osmotic pressure over the tissue at early treatment, leading to a fast dehydration of the tissue sample. This way, the fast rise observed at the beginning for this treatment corresponds only to the water flux out of the tissue. From Fig. 5, we see that the diffusion time that corresponds to the concentration of 60% of EG in solution is 57.9 s. In our previous study with glucose solutions,[33] we have determined a diffusion time of 58.4 s for water with a treatment with glucose 54% (also represented in Fig. 5), which is the maximum concentration possible for glucose in aqueous solution due to its solubility in water. As we can see, the diffusion time values of water in the muscle obtained from both treatments are very similar. Considering the value obtained with the EG study, we have used Eq. (2) to calculate the diffusion coefficient for water in the skeletal muscle:

$$D_{\text{water}} = \frac{d^2}{\pi^2 \tau_{\text{water}}} = \frac{0.0422^2}{\pi^2 \times 57.9} = 3.12 \times 10^{-6} \text{ cm}^2/\text{s}. \quad (9)$$

The thickness value $d$ used in Eq. (9) is the thickness of the sample obtained for 57.9 s in a treatment with EG 60%. For the treatment with glucose 54%, we have obtained a sample thickness of 0.0431 cm for 58.4 s of treatment. These values used in Eq. (9) give a diffusion coefficient for water relative to glucose treatments of $3.22\times10^{-6}$ cm$^2$/s. Again, we see that the diffusion coefficient values obtained for water from the two treatments are very similar.

This value is almost three times less than the diffusion coefficient of water in water at 20°C, i.e., $D_{\text{water/water}} = 8.9\times10^{-6}$ cm$^2$/s at 20°C.[39] Considering that a soft tissue contains a considerable amount of water, the diffusion of water molecules in water is a good model for water diffusion in tissues. A threefold decrease of the diffusion rate of water in muscle tissue compared with its diffusion in water can be explained by a hidden diffusion due to water molecules interaction with organic matrix and limited cell membrane permeability.

Such data are very important to understand and characterize the dehydration and the RI matching mechanisms involved in optical clearing of the skeletal muscle.

Considering the diffusion coefficient of EG, glucose, and water in muscle, we can make some comparison with other values published in literature. For instance, the diffusion coefficient of EG in water is $1.16\times10^{-5}$ cm$^2$/s at 25°C.[40] Despite the temperature difference, we see that the diffusion coefficient of EG in muscle that we have calculated with Eq. (8) is approximately 25 times smaller than the value published for EG diffusion in water. Such a difference suggests that the permeability of the muscle cell membrane might significantly slow EG diffusion inside the muscle. Another more complex situation might be considered. It is known that the water also diffuses in EG. The literature indicates the diffusion coefficient of water in EG as $1.8\times10^{-6}$ cm$^2$/s at 27°C.[40] When performing the treatment of muscle with EG, we must consider that when water flows out the sample, it will certainly flow through the EG that is flowing into the muscle and this water flow toward the outside of the tissue might slow down the EG flow in.

A similar behavior might exist in the case of glucose diffusion in muscle. It is known that the diffusion coefficient of glucose in water is $5.7\times10^{-6}$cm$^2$/s (at 20°C).[40] By comparing this value with the one that we have calculated for the diffusion of glucose in muscle ($5.90\times10^{-7}$ cm$^2$/s), we see that in muscle, glucose has a diffusion coefficient approximately 10 times smaller than in water at the same temperature. This fact is an additional indication that both EG and glucose diffusions in muscle are limited by muscle cell membrane permeability and possibly the water diffusion through these agents might also contribute to slow their diffusion into the muscle.

## 4 Conclusions

Considering the results that we have obtained with this study, we can now characterize both the mechanisms of optical clearing of the skeletal muscle—tissue dehydration and RI matching. The diffusion time values obtained for water and EG indicate that the dehydration mechanism occurs in a short time period at the beginning of the optical clearing treatment as a consequence of the osmotic pressure created by the EG in the immersion solution. The same conclusion was obtained from the glucose study, where we have obtained a very similar diffusion time for water involved in the dehydration mechanism of optical clearing.[33] The RI matching mechanism takes more time to occur than the dehydration mechanism.

The method that we have used is simple and allows one to estimate both the diffusion time and the diffusion coefficient for water and EG inside the muscle. These characteristics are most valuable for optical clearing studies, but they are also important for other fields of research and clinical procedures, as we have already indicated. The method used in the present study can be applied to evaluate the diffusion characteristics of other agents, such as medications or metabolic products, in muscle or in other tissue samples. From the results obtained in the present study, we were able to identify the free water content of the skeletal muscle as 59.5%, which is the same value obtained from the glucose study.[33]

It is our commitment to continue this kind of research and we will use this simple method to perform other studies with other OCAs and with other biological tissues to estimate the characteristic diffusion properties in each case.

### Acknowledgments

The authors would like to thank the following institutions for their help in the instrumental resources made available and in the preparation of the tissue samples to perform the present research: CIETI—Centro de Inovação em Engenharia e Tecnologia Industrial, ISEP—Instituto Superior de Engenharia do Porto, Portugal, and LAIMM—Laboratório de apoio à Investigação em Medicina Molecular, Departamento de Biologia Experimental, Faculdade de Medicina da Universidade do Porto, Portugal. VVT is grateful for the support by Russian Presidential Grant NSh-703.2014.2, the Government of the Russian Federation (Grant 14.Z50.31.0004) to support scientific research projects implemented under the supervision of leading scientists, and FiDiPro, TEKES Program (40111/11), Finland.

### References

1. E. A. Genina, A. N. Bashkatov, and V. V. Tuchin, "Glucose-induced optical clearing effects in tissues and blood," in *Handbook of Optical Sensing of Glucose in Biological Fluids and Tissues*, V. V. Tuchin, Ed., pp. 657–692, CRC Press, Taylor & Francis Group, Boca Raton, Florida (2009).
2. V. V. Tuchin, *Tissue Optics: Light Scattering Methods and Instruments for Medical Diagnosis*, 2nd ed., PM 166, SPIE Press, Bellingham, Washington (2007).
3. G. Vargas et al., "Use of an agent to reduce scattering in skin," *Lasers Surg. Med.* **24**, 133–141 (1999).
4. H. Q. Zhong et al., "Quantification of glycerol diffusion in human normal and cancer breast tissues in vitro with optical coherence tomography," *Laser Phys. Lett.* **7**, 315–320 (2010).
5. I. V. Larina et al., "Enhanced OCT imaging of embryonic tissue with optical clearing," *Laser Phys. Lett.* **5**, 476–479 (2008).
6. A. N. Bashkatov, E. A. Genina, and V. V. Tuchin, "Optical immersion as a tool for tissue scattering properties control," in *Perspectives in Engineering Optics*, K. Singh and V. K. Rastogi, Eds., pp. 313–334, Anita Publications, New Delhi, India (2002).
7. E. A. Genina, A. N. Bashkatov, and V. V. Tuchin, "Tissue optical immersion clearing," *Expert Rev. Med. Devices* **7**(6), 825–842 (2010).
8. E. A. Genina et al., "Light-tissue interaction at optical clearing," in *Laser Imaging and Manipulation in Cell Biology*, F. S. Pavone, Ed., pp. 115–164, Wiley-VCH Verlag GmbH & Co. KGaA, Weinheim, Germany (2010).
9. H. U. Dodt et al., "Ultramicroscopy: three-dimensional visualization of neuronal networks in the whole mouse brain," *Nat. Methods* **4**(4), 331–336 (2007).
10. A. Ertürk et al., "Three-dimensional imaging of the unsectioned adult spinal cord to assess axon regeneration and glial responses after injury," *Nat. Med.* **18**, 166–171 (2011).
11. K. Becker et al., "Chemical clearing and dehydration of GFP expressing mouse brains," *PLoS One* **7**(3), e33916 (2012).

12. K. Becker et al., "Dehydration and clearing of whole mouse brains and dissected hippocampi for ultramicroscopy," *Cold Sping Harb. Protoc.* **2013**(7), 683–684 (2013).
13. H. Hama et al., "Scale: a chemical approach for fluorescence imaging and reconstruction of transparent mouse brain," *Nat. Neurosci.* **14**, 1481–1488 (2011).
14. D. Zhu et al., "Recent progress in tissue optical clearing," *Laser Photonics Rev.* **7**(5), 732–757 (2013).
15. D. Zhu, Q. Luo, and V. V. Tuchin, "Tissue optical clearing," in *Advanced Biophotonics: Tissue Optical Sectioning*, R. K. Wang and V. V. Tuchin, Eds., pp. 621–672, CRC Press, Taylor & Francis Group, Boca Raton, Florida (2013).
16. C. Leahy, H. Radhakrishnan, and V. J. Srinivasan, "Volumetric imaging and quantification of cytoarchitecture and myeloarchitecture with intrinsic scattering contrast," *Biomed. Opt. Express* **4**(10), 1978–1990 (2013).
17. K. Chung et al., "Structural and molecular interrogation of intact biological systems," *Nature* **497**, 332–337 (2013).
18. V. V. Tuchin, *Optical Clearing of Tissues and Blood*, SPIE Press, Bellingham, Washington (2006).
19. M. G. Ghosn et al., "Differential permeability rate and percent clearing of glucose in different regions in rabbit sclera," *J. Biomed. Opt.* **13**, 021110 (2008).
20. Q. L. Zhao et al., "Quantifying glucose permeability and enhanced light penetration in ex vivo human normal and cancerous esophagus tissues with optical coherence tomography," *Laser Phys. Lett.* **8**, 71–77 (2011).
21. A. N. Bashkatov et al., "Glucose and mannitol diffusion in human dura matter," *Biophys. J.* **85**, 3310–3318 (2003).
22. H. Ullah, E. Ahmed, and M. Ikram, "Monitoring of glucose levels in biological tissues with noninvasive optical methods," *Laser Phys.* **24**, 025601 (2014).
23. O. Zhernovaya, V. V. Tuchin, and M. Leahy, "Blood optical clearing study by optical coherence tomography," *J. Biomed. Opt.* **18**(2), 026014 (2013).
24. P. Liu et al., "Discrimination of dimethyl sulfoxide diffusion coefficient in the process of optical clearing by confocal micro-Raman spectroscopy," *J. Biomed. Opt.* **18**, 020507 (2013).
25. R. Bertram and M. Pernarowski, "Glucose diffusion in pancreatic islets of Langerhans," *Biophys. J.* **74**, 1722–1731 (1998).
26. A. C. Ribeiro et al., "Binary mutual diffusion coefficients of aqueous solutions of sucrose, lactose, glucose, and fructose in the temperature range from (298.15 to 328.15) K," *J. Chem. Eng. Data* **51**, 1836–1840 (2006).
27. M. G. Ghosn et al., "Concentration effect on the diffusion of glucose in ocular tissues," *Opt. Laser Eng.* **46**, 911–914 (2008).
28. O. Nadiamykh and P. J. Campagnola, "SHG and optical clearing," in *Second Harmonic Generation Imaging*, F. S. Pavone and P. J. Campagnola, Eds., pp. 169–189, CRC Press, Taylor & Francis Group, Boca Raton, Florida (2014).
29. M. M. Stolnitz et al., "Mathematical modeling of clearing liquid penetration into the skin," in *Saratov Fall Meeting 2006: Optical Technologies in Biophysics and Medicine*, V. V. Tuchin, Ed., Vol. 6535, pp. 653520, SPIE Press, Bellingham, Washington (2007).
30. V. V. Tuchin et al., "Light propagation in tissues with controlled optical properties," *J. Biomed. Opt.* **2**, 401–417 (1997).
31. A. Kotyk and K. Janacek, *Membrane Transport: An Interdisciplinary Approach*, Plenum Press, New York (1977).
32. M. Kreft et al., "Diffusion of D-glucose measured in the cytosol of a single astrocyte," *Cell. Mol. Life Sci.* **70**(8), 1483–1492 (2013).
33. L. M. Oliveira et al., "The characteristic time of glucose diffusion measured for muscle tissue at optical clearing," *Laser Phys.* **23**, 075606 (2013).
34. S. R. White, "Toxic alcohols," in *Rosen's Emergency Medicine: Concepts and Clinical Practice*, J. A. Marx, R. S. Hockberger, and R. M. Walls, Eds. Vol. 2, 7th ed., pp. 2001–2009, Elsevier, Philadelphia, Pennsylvania (2010).
35. M. Toledo, "Ethylene glycol–Refractometry concentration table (+20 ºC)," http://us.mt.com/us/en/home/supportive_content/application_editorials/Ethylene_Glycol_re_e.html (22 November 2013).
36. R. C. Haskell, F. D. Carlson, and P. S. Blank, "Form birefringence of muscle," *Biophys. J.* **56**, 401–413 (1989).
37. R. F. Reinoso, B. A. Telfer, and M. Rowland, "Tissue water content in rats measured by dissecation," *J. Pharmacol. Toxicol. Methods* **38**, 87–92 (1997).
38. P. Ballard, D. E. Leahy, and M. Rowland, "Prediction of in vivo tissue distribution from in vitro data 1. Experiments with markers of aqueous spaces," *Pharm. Res.* **17**(6), 660–663 (2000).
39. I. K. Kikoin, Ed., *Handbook of Physical Values*, Atomizdat, Moscow (1976).
40. I. S. Grigor'ev and E. Z. Meilikov, Eds., *Handbook of Physical Values*, Energoatomizdat, Moscow (1991).

**Luís M. Oliveira** graduated in physics at Porto University, Portugal in 2000 and received MSc and PhD degrees in biomedical engineering from Porto University in 2007 and 2014, respectively. He is currently a lecturer at the Physics Department of the Polytechnic of Porto—School of Engineering and a biomedical optics researcher at the Center for Innovation in Engineering and Industrial Technology (CIETI), Portugal. His main research area is tissue optics, including optical clearing.

**Maria Inês Carvalho** graduated in electrical and computer engineering at Porto University, Portugal, in 1990, and received MSc and PhD degrees in electrical engineering from Lehigh University, USA, in 1994 and 1996, respectively. She is currently an associate professor in electrical engineering at Porto University, and a senior researcher at INESC TEC, Portugal. Her main research area is electromagnetic wave propagation, including nonlinear effects in communications technologies and biomedical optics.

**Elisabete M. Nogueira** received a MSc degree in electrical and computer engineering at Porto University (1992) and a PhD degree in applied physics at Minho University (2000). She is currently an associate professor and head of the Physics Department at Polytechnic of Porto (Portugal)—School of Engineering, and a senior researcher at the Center for Innovation in Engineering and Industrial Technology (CIETI). Her research interests include acoustic propagation in human tissues (including cancer) nanomaterials and biomedical optics.

**Valery V. Tuchin** is a director of Research-Educational Institute of Optics and Biophotonics, Saratov State University. He has authored more than 350 peer-reviewed papers and books, awarded Russian Honored Science Worker, SPIE Fellow, the SPIE Educator Award, and Chime Bell Prize of Hubei Province, China. He is a FiDiPro Professor of University of Oulu (Finland), guest professor of HUST (Wuhan) and Tianjin Universities of China, and adjunct professor of the National University of Ireland (Galway).